



## STOCHASTIC FINITE ELEMENT ANALYSIS OF PORTUGUESE ADOBE MASONRY

F. Parisi<sup>(1)</sup>, C. Balestrieri<sup>(2)</sup>, H. Varum<sup>(3)</sup>

<sup>(1)</sup> Assistant Professor, Department of Structures for Engineering and Architecture, University of Naples Federico II, Via Claudio 21, 80125 Naples, Italy, [fulvio.parisi@unina.it](mailto:fulvio.parisi@unina.it)

<sup>(2)</sup> Research Fellow, Department of Structures for Engineering and Architecture, University of Naples Federico II, Via Claudio 21, 80125 Naples, Italy, [claudiobalestrieri@gmail.com](mailto:claudiobalestrieri@gmail.com)

<sup>(3)</sup> Full Professor, CONSTRUCT-LESE, Department of Civil Engineering, Faculty of Engineering of the University of Porto, R. Dr. Roberto Frias, 4200-465 Porto, Portugal, [hvarum@fe.up.pt](mailto:hvarum@fe.up.pt)

### **Abstract**

Earth is a construction material which has been used since ancient times in many parts of the world according to its local availability, low manufacturing cost, and its need for simple construction techniques. Even though earthen constructions have good thermo-acoustic properties, they typically show a very poor performance under earthquake ground motion. Rammed earth and adobe masonry are the main types of earthen construction. Nowadays, it is estimated that approximately 30% of the world population lives in earthen buildings and this percentage increases up to around 50% in developing countries. Such an information highlights the need for a seismic assessment and strengthening of existing earthen structures. The present study is focused on the mechanical behavior of the traditional adobe masonry (AM) of the Aveiro district, Portugal, where approximately 40% of existing buildings are made of adobe and many of them have a socio-cultural value. Extensive surveys have shown a poor state of conservation of AM buildings, the strengthening of which should be based on a comprehensive knowledge of mechanical properties and behavior. To that aim, a nonlinear finite element (FE) modelling approach is used to simulate the experimental behavior of AM in different boundary and loading conditions associated with axial and diagonal compression tests. The latter are amongst the most common experimental tests used for mechanical characterization of masonry assemblages, particularly to define their macroscopic response to uniaxial compression and shear. Based on statistics for mechanical properties of adobe bricks and mud mortar provided by past experimental tests, a macromechanical model of AM was developed within LS-DYNA software and validated against experimental data. The FE models of two types of specimens subjected to axial compression and diagonal compression, separately, were generated. A comparative analysis between numerical and experimental results, both in terms of force–displacement curves and crack patterns, showed that the FE model was able to reproduce the real behavior of AM in different boundary and loading conditions. Afterwards, a single-parameter sensitivity analysis was performed on each AM model to assess whether and how the AM behavior changes under varying material properties. That analysis was the basis for a probabilistic assessment in which a stochastic FE analysis was carried out. Each material property was assumed to be a spatially-distributed random variable in order to reproduce the high level of inhomogeneity provided by material tests on AM constituents, that is adobe bricks and mortar. A small number of model realizations subjected to axial compression was randomly generated through Monte Carlo simulation technique. Two alternative types of stochastic representation were adopted. The former was a simplified stochastic FE modeling (SFEM) in which the spatial variability of material properties was lumped into single brick units, each of them fictitiously extended to the middle of mortar joints. In the second case, an advanced stochastic FE modeling (ASFEM) strategy was used and consisted in a random generation of material properties for all finite elements. It was found that even a limited number of ASFEM simulations allowed the experimental force–displacement response to be captured.

*Keywords: adobe masonry; nonlinear macromechanical finite element modeling; experimental validation; sensitivity analysis; stochastic finite element analysis.*



## 1. Introduction

Adobe masonry (AM) is one of the most largely used construction materials worldwide due to local availability of constituent materials, low manufacturing cost, simple construction technique and good thermo-acoustic properties. AM is a masonry assemblage consisting of adobe bricks and mud mortar [1]. The bricks are typically produced by pressing a mixture of soil, water and reinforcing fibers (either natural or artificial) into a prismatic formwork, and then drying each brick by means of the combined action of air and sunshine. In some cases, the mixture of adobe bricks is stabilized through additives such as lime and cement. Together with rammed earth, AM falls in the class of earthen construction materials that have been used in various historical ages and countries, starting at least 5000 years ago in Mesopotamia and Turkmenistan. In this respect, approximately 10% of the UNESCO World Heritage properties consists of earthen constructions, including European historical cities such as Guimarães, Oporto, Cordoba and Lyon. Even nowadays, it is observed a growing interest in new earthen structures to ensure a sustainable development of both urban and rural centers, comfort to building occupants, and architectural compatibility with historical built environments. This also occurs in countries such as Italy, where several examples of earthen buildings are still present, especially in Piemonte, Marche, Abruzzo, Emilia Romagna and Sardinia. In some less developed regions of Africa, Asia and Latin America, earthen materials are typically used to build nonengineered constructions, resulting in informal urban settlements with significant vulnerability to natural hazards (e.g. earthquakes, floods, landslides). Such observations are consistent with the fact that a large fraction of world population lives in earthen constructions. These statistics motivated an increasing number of research studies on AM constructions. Most of studies focused on seismic response and strengthening of AM constructions (see e.g. [2]–[6]). An extensive research was conducted at the Pontifical Catholic University of Peru (PUCP), starting between 1970s and early 1980s, and focusing on mechanical properties and structural behavior of Peruvian AM constructions [7]. More recently, material properties and structural response of AM buildings were further investigated by several scholars, allowing a worldwide database on mechanical properties of adobe bricks to be developed. In Portugal, AM was commonly used until the middle of the 20th century and the Aveiro district is an emblematic region where approximately 40% of the building stock is composed of AM structures. Most of those buildings present an important cultural, social and architectural value, but at the same time a poor state of conservation and structural deficiencies. Therefore, on one hand a mechanical characterization of traditional AM of Aveiro district needs to be performed and on the other an experimental and numerical assessment of AM buildings in view of their seismic strengthening. Based on a past experimental campaign by Silveira et al. [8], the authors of this paper carried out a numerical investigation aimed at developing a robust nonlinear finite element (FE) model for Aveiro's AM.

## 2. Research methodology

A macromechanical FE model of the case-study AM was developed in LS-DYNA software [9] by using the soil-and-foam material model developed by Krieg [10]. A homogeneous model is adopted according to the very similar values of mechanical properties of adobe bricks and mud mortar in the case of Aveiro's AM [8]. The soil-and-foam material model was employed because it produced successfully results for different masonry types [11][12]. Furthermore, that material model has a considerable amount of use experience, needing few input data to define the mechanical behavior and being generally applied to crushable foams and geomaterials (e.g. rock, soil, concrete). In those materials, compressibility is relatively high, yield strength depends on the mean stress, and tensile strength is significantly smaller than compressive strength. After that appropriate values were assigned to strengths and elastic moduli of AM, the mechanical behaviour was simulated in different boundary and loading conditions corresponding to the axial and diagonal compression tests presented in [8]. The specimens consisted of earth block masonry wallettes with mud mortar. The validation of the nonlinear FE model was based on an experimental-numerical comparison in terms of load–displacement diagrams and crack patterns. The numerical robustness of the FE model was validated in two boundary and loading conditions related to axial and diagonal compression laboratory tests. A sensitivity analysis was performed to evaluate variations in model response as single material properties change according to their statistical variability. Finally, the inhomogeneity of AM was probabilistically modeled through spatially distributed material properties.

### 3. Experimental database

Experimental data on physical and mechanical properties of AM were collected from Silveira et al. [8]. Those researchers carried out axial and diagonal compression tests on ten full scale AM wallettes that were constructed in laboratory with adobe bricks extracted from existing constructions in the Aveiro district and with mortar having a traditional composition. Five specimens were tested under axial compression and other specimens were tested in diagonal compression. Figures 1a and 1b show respectively the experimental setup and load–displacement curves of specimens subjected to axial compression tests. Similarly, Figures 2a and 2b show the setup and load–displacement curves related to diagonal compression tests.

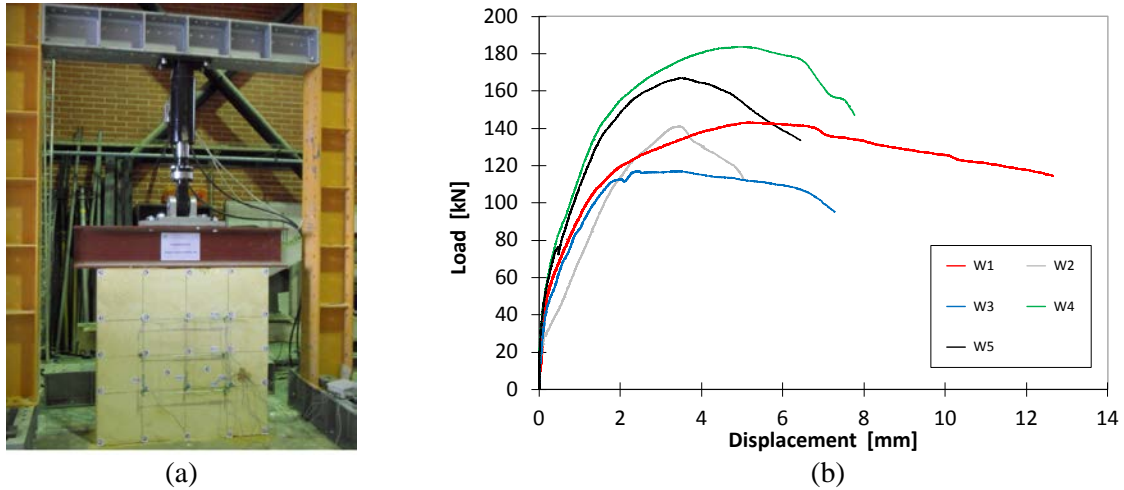


Fig. 1 – Uniaxial compression tests: (a) experimental setup; (b) load–displacement curves

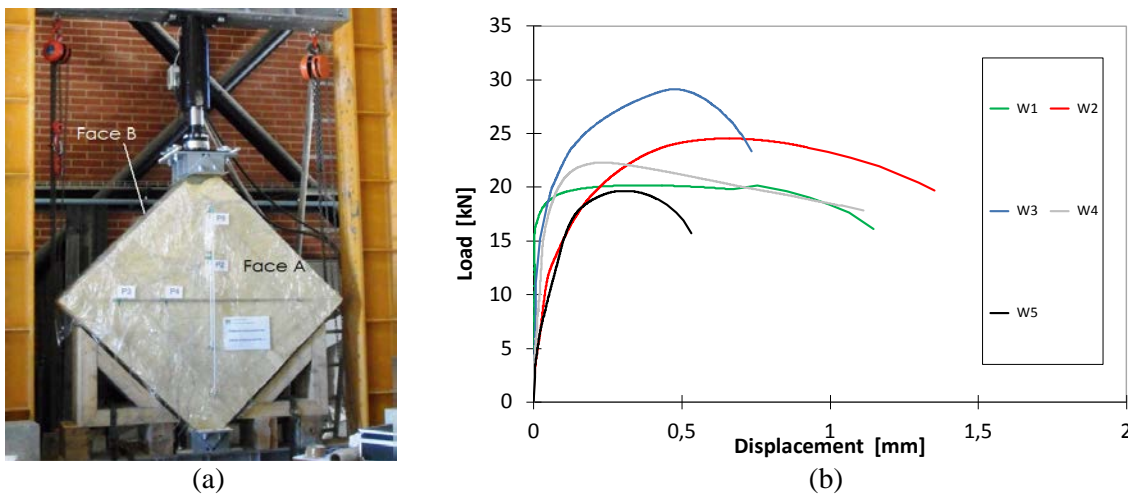


Fig. 2 – Diagonal compression tests: (a) experimental setup; (b) load–displacement curves

Experimental tests were carried out with displacement control and AM specimens experienced a quasibrittle behavior. All specimens were  $1260 \times 1260 \times 360 \text{ mm}^3$  in size and were characterized by a running bond scheme and two leaves. Adobe bricks were  $460 \times 320 \times 120 \text{ mm}^3$  in size and mortar joints were 20 mm-thick. The adobe bricks had the following characteristics: mean unit weight of  $15 \text{ kN/m}^3$  (coefficient of variation  $\text{CoV} = 5\%$ ), mean compressive strength  $f_c = 0.466 \text{ MPa}$  ( $\text{CoV} = 34\%$ ), mean Young’s modulus  $E = 13,068 \text{ MPa}$  ( $\text{CoV} = 32\%$ ), and mean splitting tensile strength  $f_t = 0.137 \text{ MPa}$  ( $\text{CoV} = 65\%$ ). The mortar was characterized by mean unit weight of  $17 \text{ kN/m}^3$  ( $\text{CoV} = 7\%$ ) and mean compressive strength of  $0.469 \text{ MPa}$  ( $\text{CoV} = 24\%$ ). Young’s modulus of mortar was not determined as it is expected to be very close to that of adobe bricks, according to



their equal composition, production and curing process. Axial compression tests were performed with loading perpendicular to mortar bed joints. A reaction steel beam was placed above each specimen to distribute the axial compressive load (Fig. 1a). Experimental load–displacement curves are shown in Figure 1b. Diagonal compression tests were performed by applying loading through steel shoes in opposite corners of each specimen (Fig. 2a) and experimental curves are shown in Figure 2b. In all tests, relative displacements on both faces of specimens were monitored by linear variable displacement transducers (LVDTs). The damage to specimens subjected to axial compression consisted of vertical cracks which were distributed over both faces (crushing). Conversely, single diagonal cracks were observed during diagonal compression tests.

#### 4. Development and validation of numerical model

The main objective of this paper was to develop and validate a macromechanical FE model for the case-study AM through a FE software able to perform nonlinear analysis of structures. Macromodeling of adobe masonry was performed through a regular mesh of eight-node solid elements with cubic shape and 20 mm edge. The size of finite elements was equal to the thickness of mortar joints and was selected after an accurate mesh sensitivity analysis. The numerical models of the specimens tested in axial and diagonal compression was made of 63,504 elements. Single-point integration elements were used to get correct results. In this case, hourglass energy was monitored to guarantee reliable results. Among several material models available in LS-DYNA software (e.g. cap, concrete, pseudotensor, Winfrith concrete), the soil-and-foam model was selected according to previous studies that confirmed its potential of reproducing the mechanical behavior of masonry structures [11]–[12]. That material model was recently calibrated by Parisi et al. [12] for tuff stone masonry. The main physical-mechanical properties of AM used in numerical modeling are outlined in Table 1, including the mass density  $\rho$ , shear modulus  $G$  and bulk modulus  $K$ . The latter was derived according to [12]. Bracketed figures in Table 1 indicate the CoV of a material property. It is noted that splitting tests evidenced a high dispersion in tensile strength, that is 65%.

Table 1 – Physical-mechanical properties of adobe masonry

Material	$\rho$ [kg]	$G$ [MPa]	$K$ [MPa]	$f_t$ [MPa]	$f_c$ [MPa]
Adobe	1600	520 (32%)	6700	0.137 (65%)	0.466 (32%)

##### 4.1 Numerical-experimental comparisons for axial compressive loading

According to the experimental setup, all the nodes located at the base of the model were assumed to be free to move in the horizontal direction (rollers), exception made for central nodes that were hinged. All nodes located on top were loaded. Figure 3 shows that the FE model with mean properties allows a good reproduction of initial stiffness, peak resistance and softening branch, as the numerical load–displacement curve is between the experimental curves. Figure 4 shows that the spread pattern of plastic strains is compatible with that of cracks observed during testing.

Based on a preliminary sensitivity analysis, the authors found that using a FE mesh with 20 mm size allowed a good balance between computational work and numerical-experimental matching. That size was the thickness of mortar joints. By contrast, increasing the mesh size to 30 mm did not produce satisfactory results in terms of load–displacement curve. The numerical-experimental comparison was also carried out at local scale by monitoring vertical stresses in three finite elements located in the central part of the model (Fig. 5a). The numerical vertical stresses were compared to the mean compressive strength of the masonry, highlighting that approximately all selected elements reached that stress level (Fig. 5b). Therefore, such a comparison demonstrates that the numerical model with mean material properties is able to reproduce the experimental behavior and damage at both local and global scales.

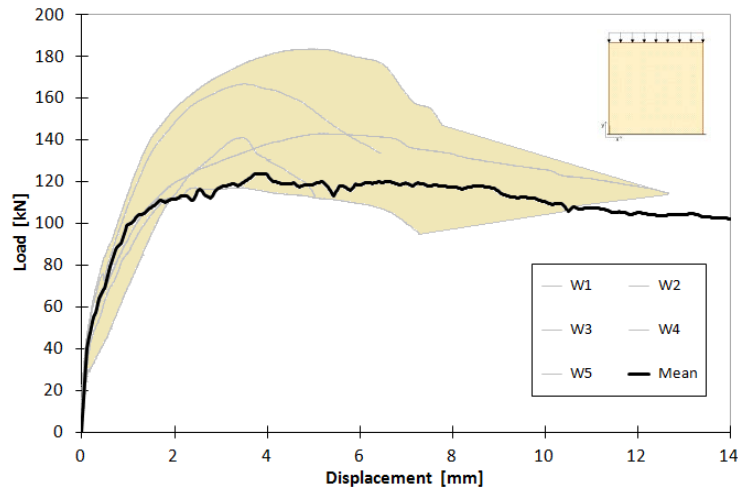


Fig. 3 – Experimental versus mean numerical load–displacement curves related to axial compression

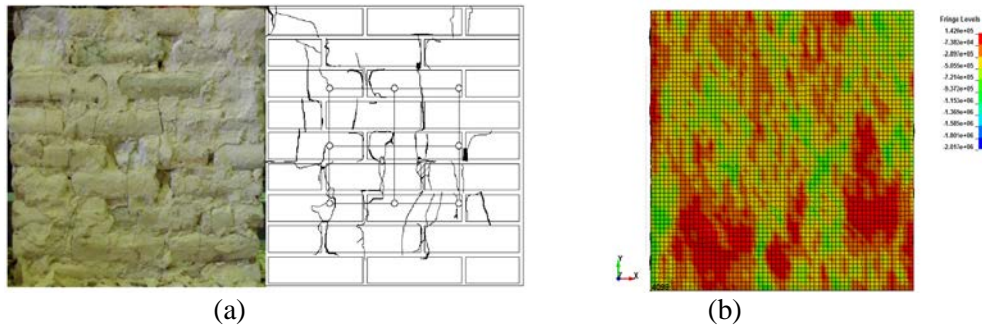


Fig. 4 – Comparison between (a) observed cracks and (b) vertical plastic strains induced by axial compression

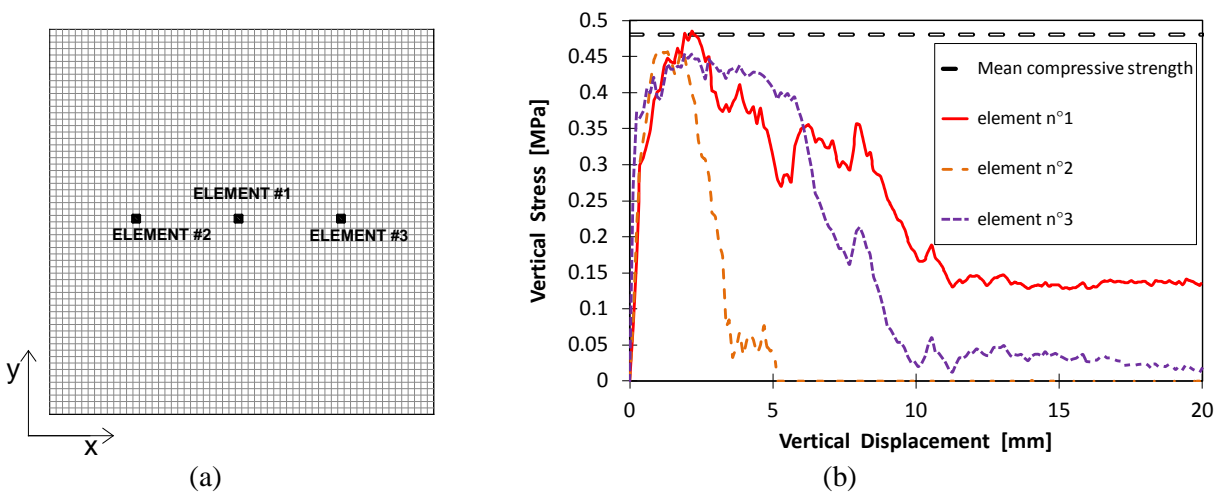


Fig. 5 – Monitoring of vertical compressive stresses in the central part of the numerical model subjected to axial compression: (a) finite elements selected; (b) comparison between vertical stresses and mean compressive strength of the case-study AM

The numerical-experimental comparison at local level was extended to vertical relative displacements measured in the central part of the numerical model with mean material properties (Fig. 6a). Experimental measurements from three couples of LVDTs named V1A, V1B, V2A, V2B, V3A and V3B were considered, in relation to faces A and B of the specimens subjected to axial compression. Experimental and numerical displacements were associated with the same points located on end sections of the middle third of the specimen and its FE model, respectively. Displacement readings of V2A and V2B were aligned with the vertical axis of symmetry. V1 and V3 couples of LVDTs were located 250 mm away from the vertical centerline. Thus, vertical displacements from the FE model and specimens were averaged (that is,  $\Delta_{V_i} = (\Delta_{V_{iA}} + \Delta_{V_{iB}})/2$  with  $i = 1,2,3$ ) and associated with the same vertical displacements imposed on top. That procedure allowed to derive the relationship between the average displacements provided by numerical analysis and those measured during testing (Fig. 6b). The model error in terms of displacements was also characterized as a Normal random variable (RV) defined as  $ME = \Delta_{EXP}/\Delta_{FEM}$ . The mean of that ratio was found to be 1.17, whereas CoV was equal to 15%.

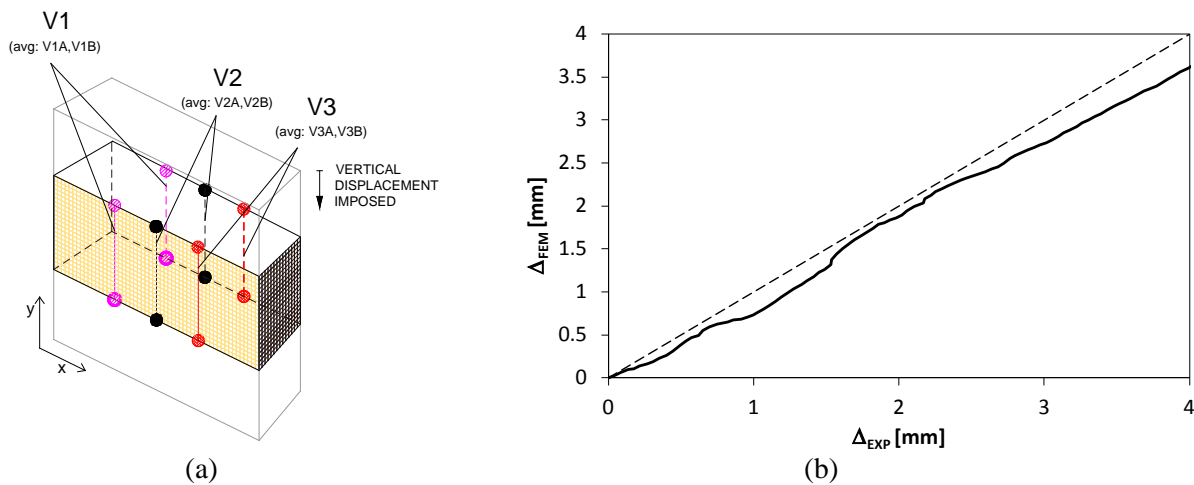


Fig. 6 – Monitoring of vertical relative displacements in the central part of the numerical model: (a) location of LVDTs and finite elements at their ends; (b) comparison between average FEM displacements and average experimental displacements

#### 4.2 Numerical-experimental comparisons for diagonal compressive loading

The numerical model used to simulate diagonal compressive behavior had equal geometry, but different boundary and load conditions with respect to the model subjected to axial compression. According to the experimental setup, all nodes located in the corner steel shoes were assumed to be hinged and those located on top were subjected to monotonically increasing vertical displacements. The FE model with mean properties reproduces fairly well the initial stiffness and peak resistance, showing a gradual strength degradation (Fig. 7). It is worth noting that an impressive simulation of the diagonal crack pattern was obtained, as highlighted in Figs. 8a and 8b. In detail, the crack pattern did not significantly affect the corners restrained by the steel shoes. Local tensile stresses in the horizontal direction of the numerical model with mean material properties were monitored as the vertical displacement on top was monotonically increased. Three finite elements were considered, including a couple of elements located at the ends of the horizontal LVDTs placed over faces A and B of the specimen (Fig. 9a). The gauge length of those LVDTs was equal to 605 mm. It was found that horizontal stresses approached the mean tensile strength of the masonry, according to the fact that masonry failure in diagonal compression may be governed by tensile failure in the transverse direction. The numerical-experimental comparison at local level was also performed in terms of horizontal displacements under varying vertical displacement on top corner of the specimen. No figures are reported in that case for the sake of brevity, but this procedure allowed the ME of the FE model subjected to diagonal compression to be estimated as in the case of axial compression. The mean and CoV of that ME in terms of horizontal displacements were 1.30 and 42%, respectively.

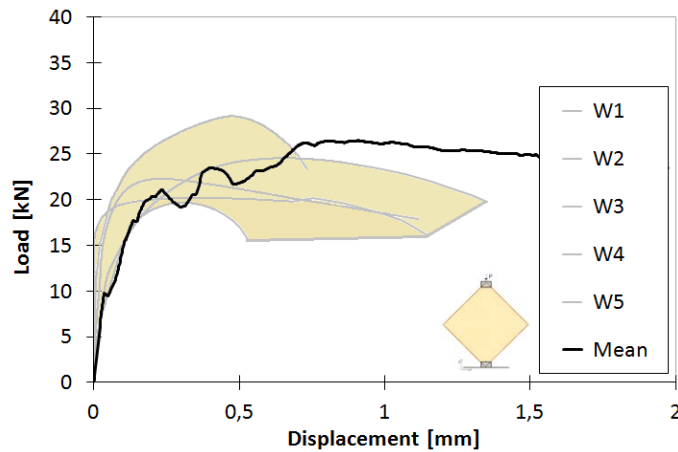


Fig. 7 – Experimental versus mean numerical load–displacement curves related to diagonal compression

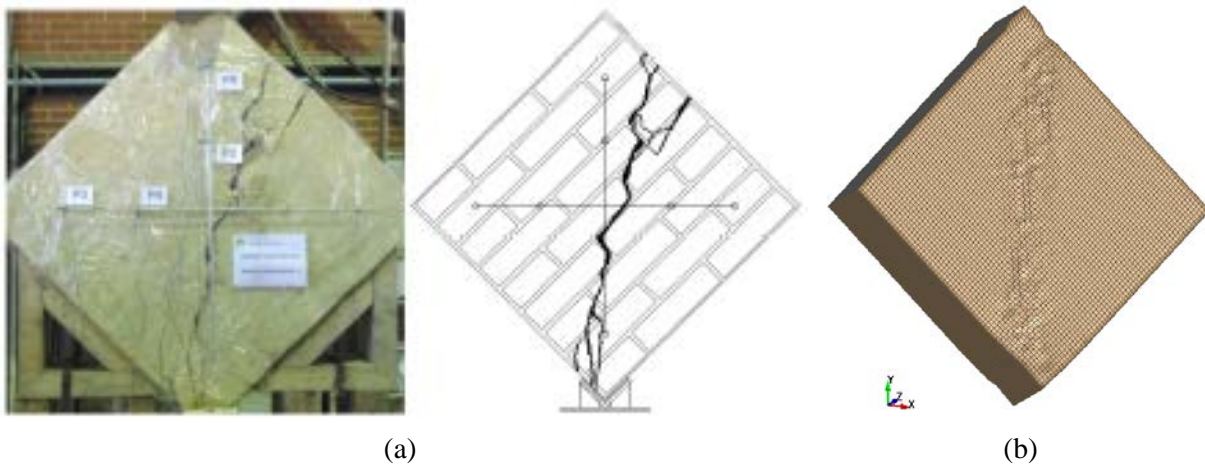


Fig. 8 – Comparison between (a) observed cracks and (b) deformed shape related to diagonal compression

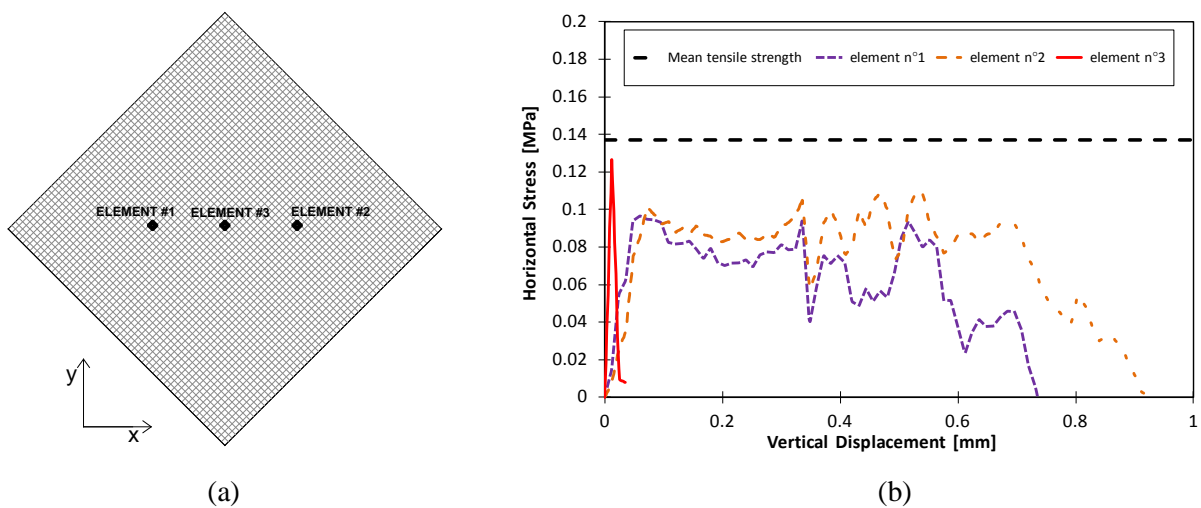


Fig. 9 – Monitoring of horizontal stresses in the numerical model subjected to diagonal compression: (a) finite elements selected; (b) comparison between horizontal stresses and mean tensile strength of the case-study AM

### 5. Sensitivity analysis of adobe masonry models

The mechanical properties that primarily affect the nonlinear behavior AM panels in axial and diagonal compression were investigated. The experimental variability of compressive strength, tensile strength and Young’s modulus was taken into account. Material properties were uniformly increased or reduced according to their CoV. In the case of axial compression, an asymmetric sensitivity of the load–displacement curve was found by reducing and increasing compressive strength of 32% (Fig. 11a). Indeed, the peak resistance reduced of 24% and increased of 46% as a result of 32% reduction and increase in  $f_c$ , respectively.

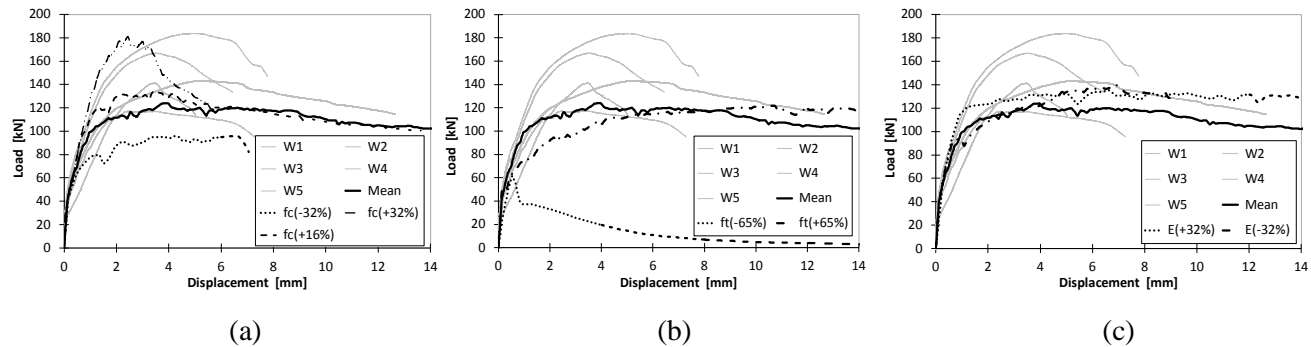


Fig. 10 – Sensitivity of axial compressive response to: (a) compressive strength, (b) tensile strength and (c) Young’s modulus

An intermediate level of increase in compressive strength, that is +16%, was considered as additional case which produced an increase in peak resistance of approximately 8%. Therefore, the experimental range of load–displacement curves was almost totally reproduced by considering a compressive strength between its mean and mean plus standard deviation. The initial stiffness was rather insensitive to  $f_c$ , whereas a more brittle behavior was found when the maximum increase in  $f_c$  (i.e. +32%) was assumed. This is compatible with more softened response of W5 specimen that sustained the highest level of axial compressive load. Small variations in the numerical load–displacement curve were obtained when tensile strength was increased of up to 65% (Fig. 11b). In that case, a more gradual attainment of peak resistance at larger displacements was basically the only difference between the load–displacement curve corresponding to the highest level of tensile strength and that related to mean properties. A significant reduction in peak resistance (i.e. –50%) was found when  $f_t$  was reduced of 65%, also showing a lower level of initial stiffness and brittle behavior. A 32% increase in Young’s modulus induced a stiffer prepeak response, resulting in higher peak resistance (Fig. 11c). Almost the same increase was found when  $E$  was reduced of 32%, but the prepeak response was characterized by a lower stiffness as expected. Figs. 12a–c show variations in load–displacement curves related to diagonal compressive loading. As  $f_c$  was increased of 32%, peak resistance increased approximately of 19% (Fig. 12a). Conversely, a 29% reduction in peak resistance was found when  $f_c$  was decreased.

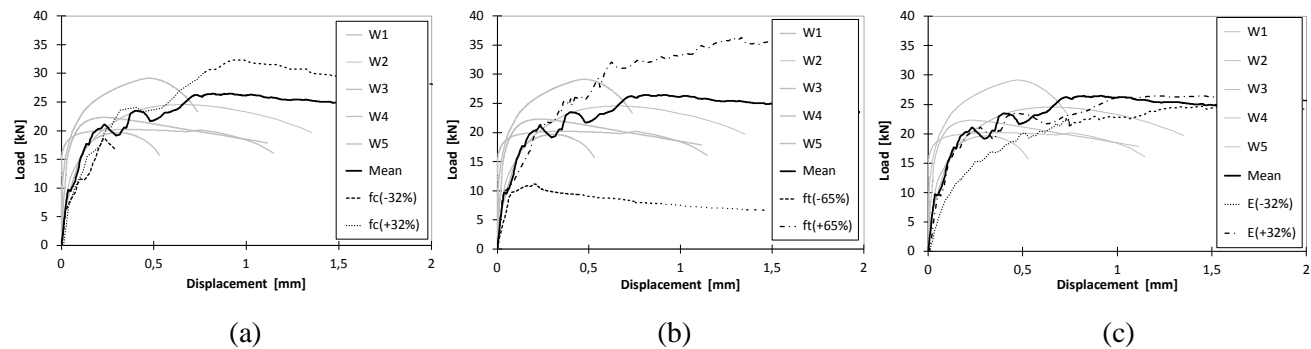


Fig. 11 – Sensitivity of diagonal compressive response to: (a) compressive strength, (b) tensile strength and (c) Young’s modulus



Tensile strength also played a major role in determining the load–displacement curves under diagonal compression (Fig. 12b). As  $f_t$  was increased and reduced of 65%, peak resistance rose of about 33% and reduced approximately of 59%. Nonetheless, the overall shape of prepeak and postpeak branches of load–displacement curves did not significantly change when  $f_t$  was increased, whereas a more brittle behavior was found when  $f_t$  was reduced. Such an outcome shows that statistical variability in tensile strength of the case-study AM is too large to reproduce the dispersion in load–displacement curves. Finally, positive and negative variations in Young’s modulus produced different changes in the load–displacement curve related to diagonal compression. As  $E$  was increased, the overall behavior did not substantially deviate from that related to mean material properties. By contrast, as Young’s modulus was reduced of 32%, a substantial reduction in stiffness was found. For instance, if elastic stiffness is conventionally measured at one-third of peak diagonal compressive load, the reduction in stiffness was approximately equal to –161%.

## 6. Stochastic finite element analysis of adobe masonry models

The sensitivity analysis was the first step towards a more refined numerical investigation based on the stochastic finite element method. Material properties were then assumed to be Lognormal RVs having spatial variability within adobe masonry. That strategy was used to model the inhomogeneity of the masonry under study. Two alternative types of stochastic representations for material properties were considered as follows: simplified stochastic FE modeling (SFEM) and advanced stochastic FE modeling (AFEM). In the former, the spatial variability of material properties was lumped into single brick units, each of them fictitiously expanded to the middle of mortar joints. The latter consisted of spatially distributed material properties for all finite elements. Any set of RVs for each ‘expanded’ brick unit (in case of SFEM) or finite element (in case of AFEM) was randomly generated through Monte Carlo simulation according to the experimental CoV. In particular, the SFEM strategy led to 27 realizations of compressive strength, tensile strength and Young’s modulus, namely a number equal to that of the expanded brick units, each of them was considered as a ‘part’ of the model into LS-DYNA software. Each part was labelled through an identification code, allowing a direct association between mechanical properties of each part and their randomly generated values. Fig. 13a shows one of the random models of AM specimens subjected to axial compression in which the parts were denoted by different colors. Each brick unit was composed of 300 finite elements. A more continuous representation of spatial variability of material properties was obtained through the AFEM strategy (Fig. 13b). In that case, a total number of 63,000 realizations of RVs was randomly generated and assigned to the finite elements.

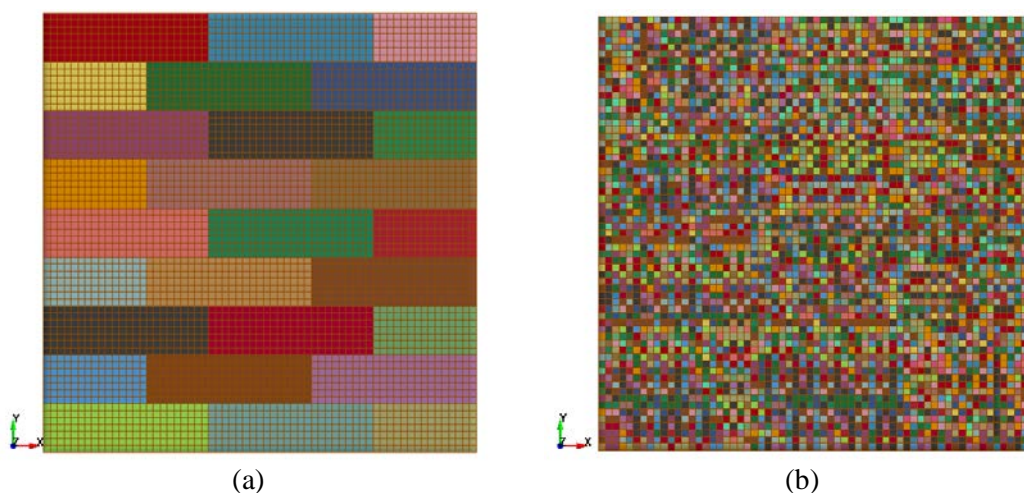


Fig. 12 – Stochastic finite element models: (a) SFEM; (b) AFEM

An interesting issue was to assess the ability of SFEM and AFEM to capture the experimental load–displacement curves through a limited number of simulations, which was set to 10. It is noted that tensile strength was assumed to have a dispersion lower than that experimentally evaluated in 65% (see Table 1). That



hypothesis was consistent with findings of previous sensibility analysis. In that respect, tensile strength was considered as a RV correlated with compressive strength, according to the study by Caporale et al. [13]. Mean tensile strength was then set to 36% of compressive strength with  $CoV = 15\%$ , given that the case-study AM was made of unreinforced adobe bricks. Figs. 14a and 14b show a comparison between experimental and numerical load–displacement curves in the cases of SFEM and AFEM, respectively. It was found that even a very small number of AFEM simulations allowed the experimental behavior to be roughly captured (Fig. 14b). That was not the case of SFEM simulations in terms of peak load (Fig. 14a), indicating that a significantly larger amount of simulations should be run.

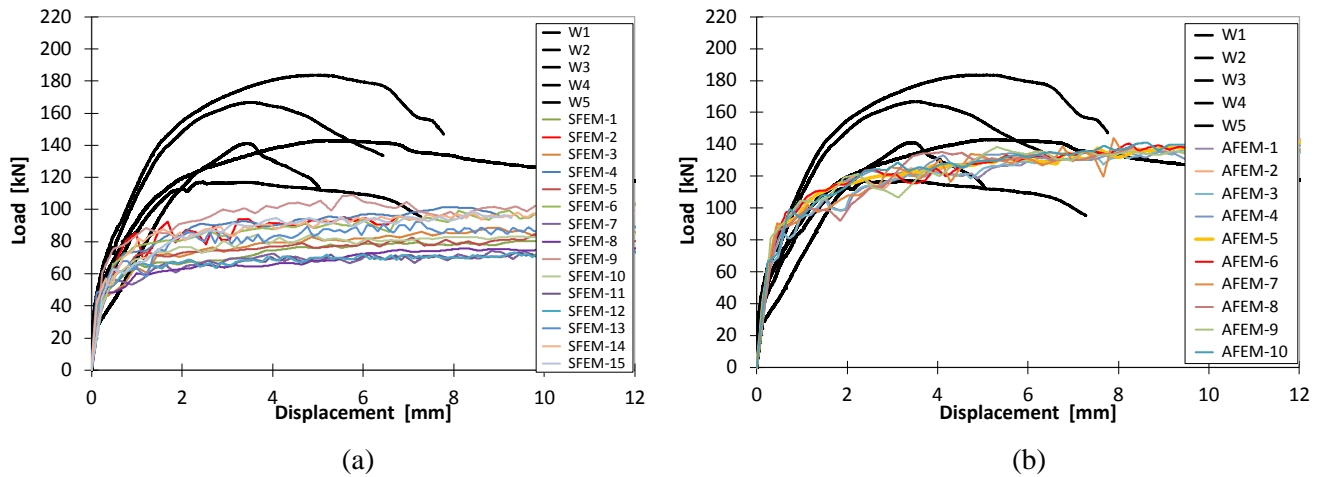


Fig. 13 – Numerical-experimental comparison between experimental and numerical load–displacement curves: (a) SFEM; (b) AFEM

## 7. Conclusions

In this study, a nonlinear macromechanical FE model of Aveiro’s adobe masonry has been proposed. The numerical model was developed on the basis of the soil-and-foam material model available in LS-DYNA software, which has been previously used to simulate the mechanical behavior of other masonry types. Material behavior was modeled according to past experimental results. The FE model was validated in two different loading and boundary conditions corresponding to axial and diagonal compression tests, in order to assess its numerical robustness. A satisfactory numerical-experimental agreement in terms of load–displacement curves and crack patterns was found. The models with mean properties allowed the initial stiffness, peak resistance and softening behavior to be reproduced fairly well. The sensitivity of load–displacement curves to compressive strength, tensile strength and Young’s modulus was investigated. The overall failure of adobe masonry was governed by compressive and tensile strengths, whereas Young’s modulus played a minor role under the loading conditions considered. Finally, the spatial variability of material properties within the adobe masonry assemblage was modeled through both simplified and advanced stochastic FE models. It was found that even a very small amount of Monte Carlo simulations integrated with the advanced stochastic modeling strategy allowed the experimental load–displacement curves to be captured. Such an outcome was not confirmed in the case of simplified stochastic models because spatial variability of material properties was lumped into a few elements, namely the expanded brick units of the masonry.

## Acknowledgments

This work was financially supported by: Project ReLUIIS-DPC 2016 (Line 1 – Masonry Structures) funded by the Italian Civil Protection Department; Project POCI-01-0145-FEDER-007457 - CONSTRUCT - Institute of R&D in Structures and Construction, funded by FEDER funds through COMPETE2020 – Programa



Operacional Competitividade e Internacionalização (POCI) – and by national funds through FCT – Fundação para a Ciência e a Tecnologia; Project "Proteção sísmica do património construído em terra", with reference POCI-01-0145-FEDER-016737 e PTDC/ECM-EST/2777/2014.

## References

- [1] Houben H, Guillaud H (1994): *Earth construction — A comprehensive guide*. Intermediate Technology Publication.
- [2] Meli R (2005): Experiences in Mexico on reducing the seismic vulnerability of adobe constructions. *SismoAdobe 2005: Architecture, construction and conservation of earthen buildings in seismic areas*, Lima, Peru.
- [3] Yamín L, Phillips C, Reyes J, Ruiz D (2007): Seismic vulnerability studies, rehabilitation and strengthening of adobe and rammed earth houses. *Apuntes*, **20**(2), 286-303.
- [4] Tolles E (2009): Getty seismic adobe project research and testing program. *Getty Seismic Adobe Project 2006 Colloquium*, Los Angeles, USA.
- [5] Blondet M, Vargas J, Tarque N, Iwaki C (2011): Earthquake-resistant earthen construction: The great contemporary experience of Pontifical Catholic University of Peru. *Informes de la Construcción*, **63**(523), 41-50.
- [6] Figueiredo A, Varum H, Costa A, Silveira D, Oliveira C (2013): Seismic retrofitting solution of an adobe masonry wall. *Materials and Structures*, **46**(1-2), 203-219.
- [7] Vargas J, Blondet M, Ginocchio F, Garcia G (2005): *35 years of research on earthquake-resistant adobe: Reinforced earth*. Pontifical Catholic University of Peru.
- [8] Silveira D, Varum H, Costa A, Carvalho J (2014): Mechanical properties and behavior of traditional adobe wall panels of the Aveiro district. *Journal of Materials in Civil Engineering*, **27**(9), 04014253.
- [9] LS-DYNA ver. 971 (2007): *User's Manual*, Livemore Software Technology Corporation.
- [10] Krieg RD (1972): A simple constitutive description for soils and crushable foams. *Report No. SC-DR-72-0883*, Sandia National Laboratories, Albuquerque, USA.
- [11] Aghdamy S, Wu C, Griffith M (2013): Simulation of retrofitted unreinforced concrete masonry unit walls under blast loading. *International Journal of Protective Structures*, **4**(1), 21-44.
- [12] Parisi F, Balestrieri C, Asprone D (2016): Nonlinear micromechanical model for tuff stone masonry: Experimental validation and performance limit states. *Construction and Building Materials*, **105**, 165-175.
- [13] Caporale A, Parisi F, Asprone D, Luciano R, Prota A (2015): Comparative micromechanical assessment of adobe and clay brick masonry assemblages based on experimental data sets. *Composite Structures*, **120**, 208-220.